Electronic Supplementary Material (ESI) for Physical Chemistry Chemical Physics.

Electronic supplementary information for

Pulse-shaped two-photon excitation of a fluorescent base analogue approaches single-molecule sensitivity

Rachel S. Fisher, David Nobis, Anders F. Füchtbauer, Mattias Bood, Morten Grøtli, L. Marcus Wilhelmsson, Anita C. Jones* and Steven W. Magennis*

*Correspondence to Prof. Anita Jones (a.c.jones@ed.ac.uk) or Dr. Steven Magennis (steven.magennis@glasgow.ac.uk)

This PDF includes:

SUPPLEMENTARY METHODS

Two-photon cross section calculations

Three two-photon cross section standards were utilised: rhodamine 6G in methanol, coumarin 153 in DMSO and coumarin 153 in toluene. These standard have been studied previously across a wide range of excitation wavelengths.[1]

2P cross-sections (σ_2) were calculated by comparison to a reference:

$$\frac{\sigma_2^S \phi^S}{\sigma_2^R \phi^R} = \frac{\eta^R n^S C^R F^S \langle P^R \rangle^2}{\eta^S n^R C^S F^R \langle P^S \rangle^2} \quad (Equation\ 1)$$

where ϕ is the quantum yield of fluorescence, η is a term that accounts for the wavelength-dependent collection efficiency of the fluorescence, n is the refractive index of the solvent, C is the concentration, F is the integrated fluorescence signal from the recorded spectrum, P is the excitation power, and the superscripts S and R refer to either the sample or reference.

Equation 1 can be rewritten as Equation 2:

$$\sigma_2^S = \frac{\alpha \sigma_2^R \phi^R n^S C^R}{\phi^S n^R C^S} \frac{F^S \langle P^R \rangle^2}{F^R \langle P^S \rangle^2} \quad (Equation\ 2)$$

where $\alpha = \frac{\eta^R}{\eta^S}$ is the correction factor for the wavelength-dependence of the detector and the second term is calculated from the slopes of the plots of integrated emission intensity (F) against power squared ($\langle P \rangle^2$) for sample and reference.

SUPPLEMENTARY FIGURES

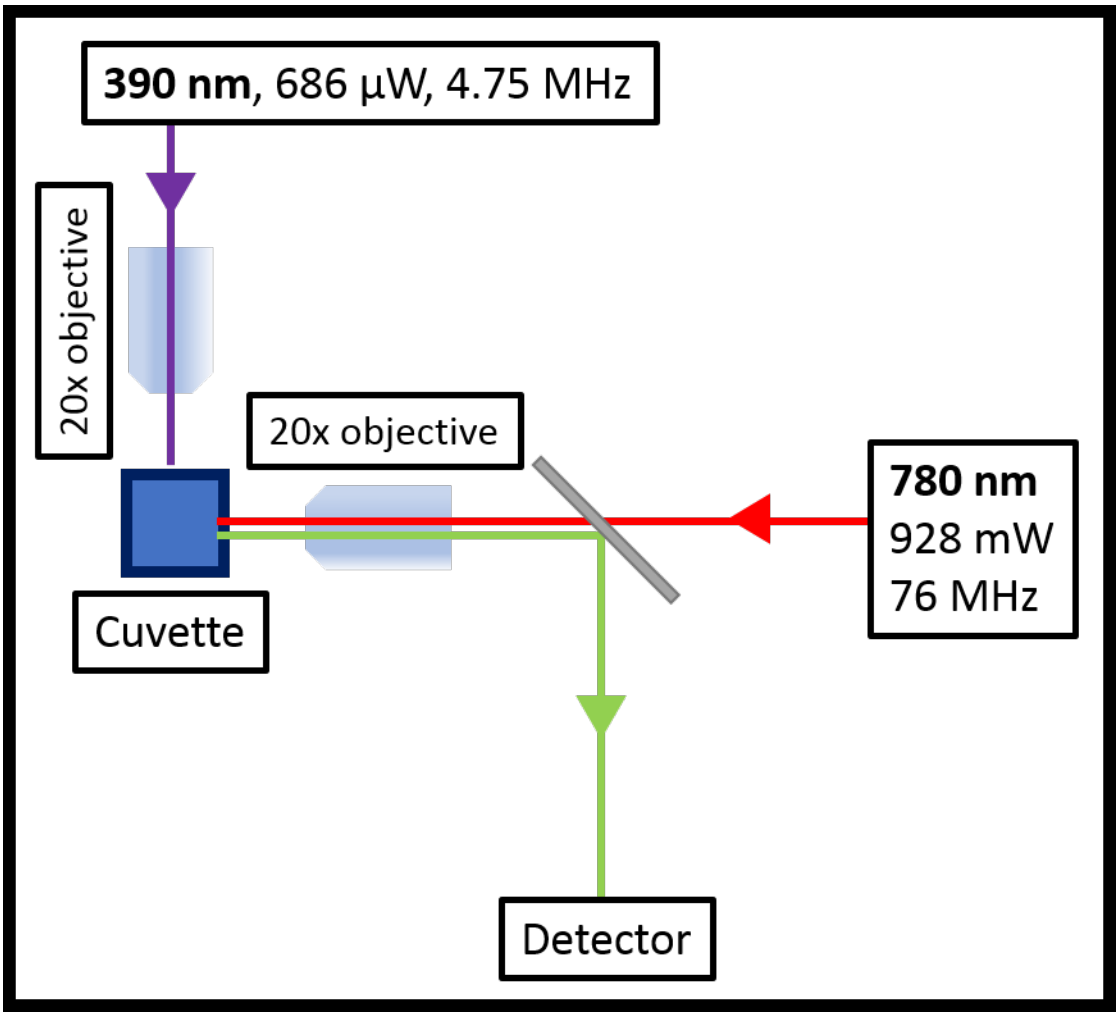

Figure S1. Schematic of experimental setup used for ensemble 2P spectroscopy and for comparison of 1P vs 2P photobleaching.

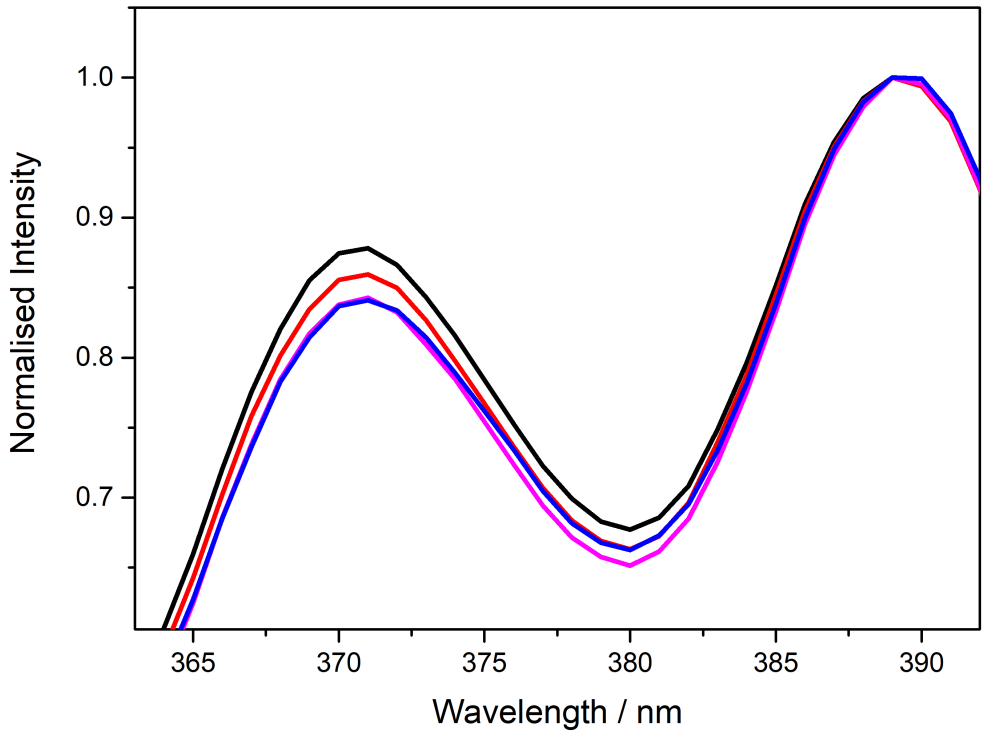

Figure S2. Normalized excitation spectra of pA riboside in ethanol, recorded at emission wavelengths of 420 nm (black), 440 nm (red), 460 nm (pink) and 480 nm (blue).

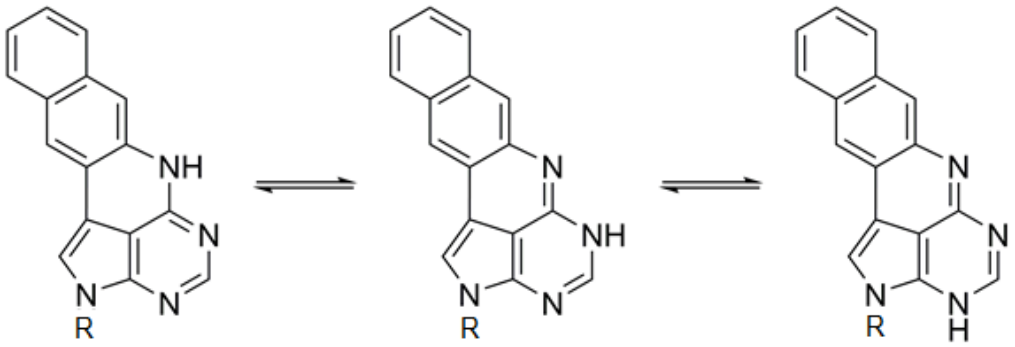

Figure S3. Structures of possible tautomeric forms of pA

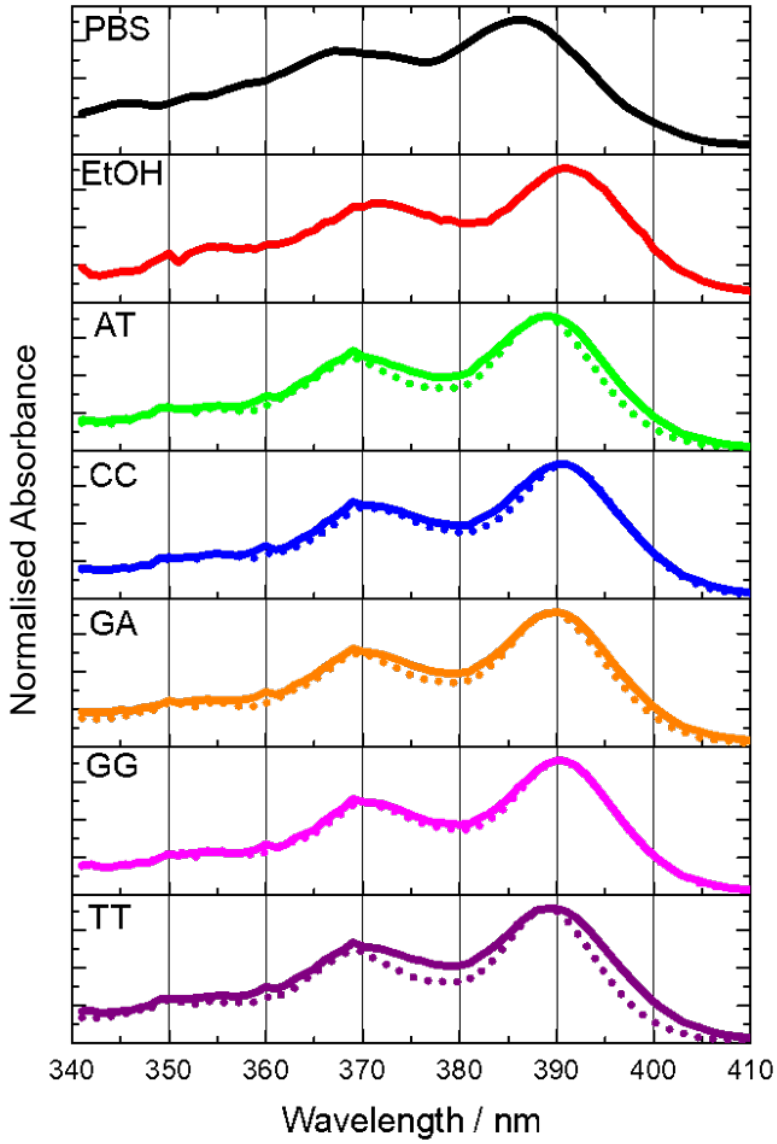

Figure S4. Absorption spectra of pA riboside in phosphate buffer at pH 7.5 (black) or ethanol (red) and pA-containing oligonucleotides with different combinations of nearest neighbours. AT (green), CC (blue), GA (cyan), GG (pink) and TT (purple). Solid line denotes single-strands and dotted line denotes double strands. In oligonucleotides CC, GA and GG, the absorption spectra of single and double strands are essentially identical. For AT and TT, a slight narrowing of the absorption bands is seen in the duplex.

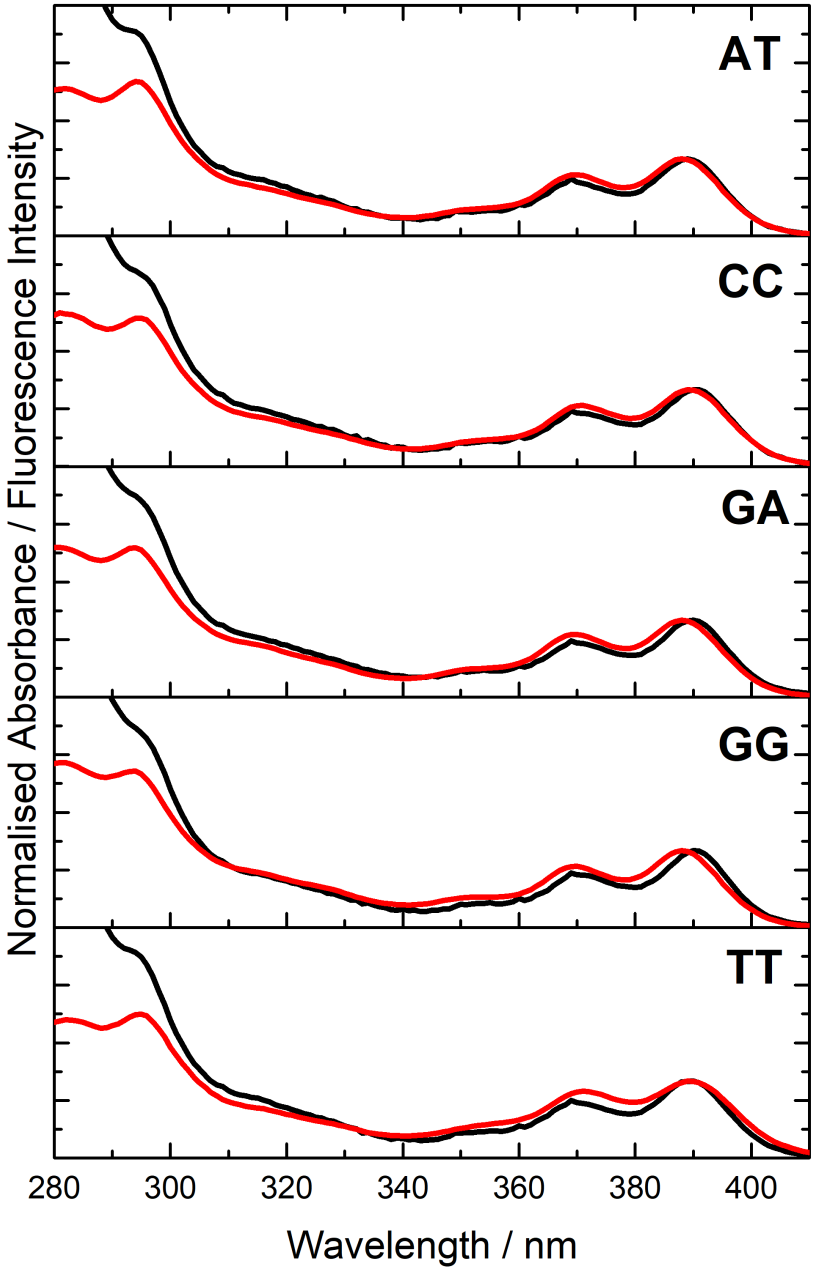

Figure S5. Comparison of excitation spectra (red), at emission wavelength 420 nm, and absorption spectra (black) of pA in single-stranded oligonucleotides with different combinations of nearest neighbours. Differences between absorption and excitation spectra below 310 nm are due to absorption by the natural bases.

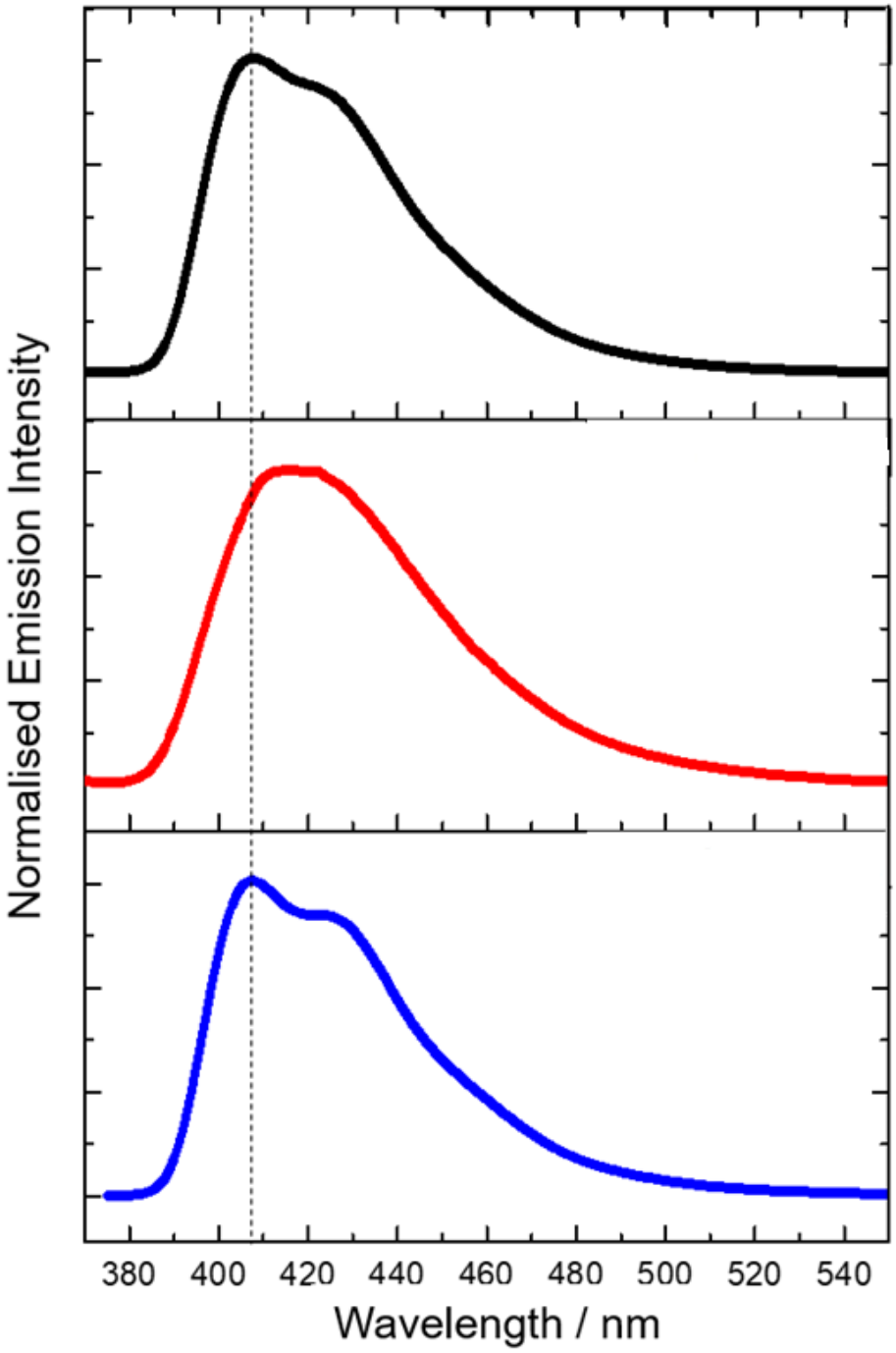

Figure S6. Normalized emission spectra of pA-containing single-stranded oligonucleotide GA, (top, black), and of pA as the free riboside in phosphate buffer at pH 7.5 (middle, red) and in ethanol (bottom, blue).

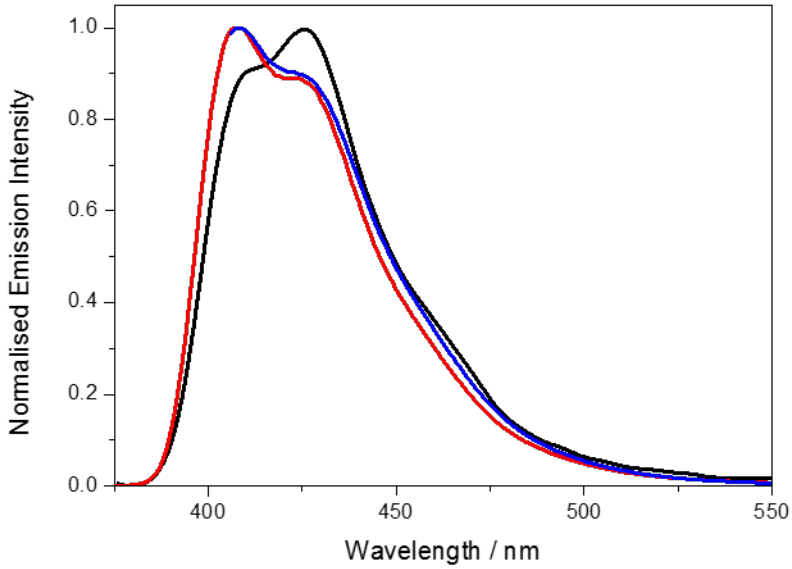

Figure S7. Normalized emission spectra of pA nucleobase in ethanol following 2P excitation at 780 nm (black), 1P excitation at 360 nm (red) and 1P excitation at 390 nm (blue)

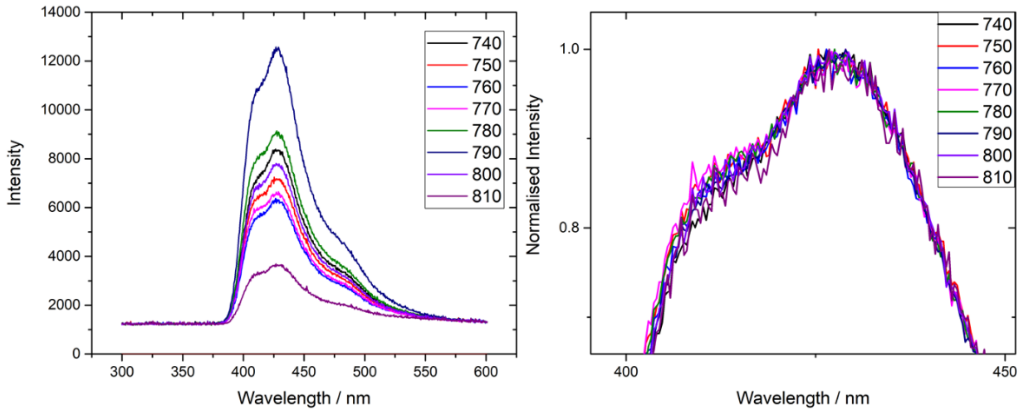

Figure S8. Emission spectra (left) and normalized emission spectra (right) for pA nucleobase in ethanol recorded at two-photon excitation wavelengths between 740 nm and 810 nm.

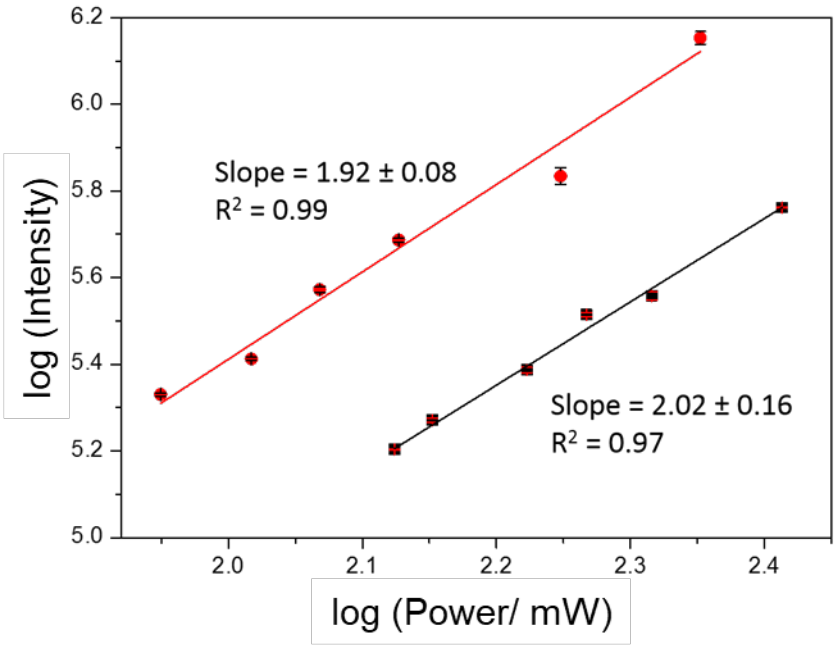

Figure S9. Log-log plot of fluorescence intensity *vs.* laser power for pA-containing GA oligonucleotides: single stranded (red), double stranded (black). Excitation wavelength was 780 nm. Laser power was varied from 90 mW to 300 mW.

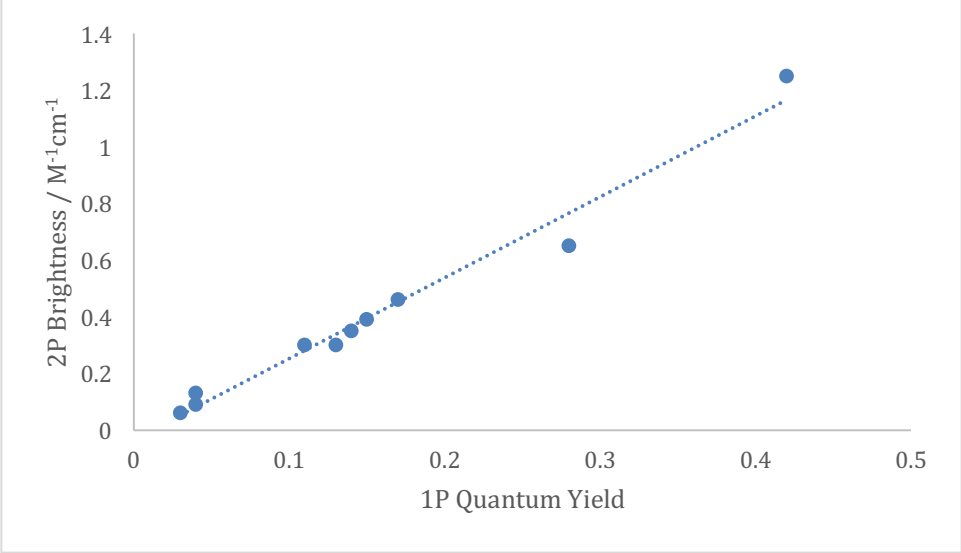

Figure S10. Correlation between 2P brightness and quantum yield measured under 1P excitation, for all pA–containing oligonucleotides, both single and double strands.

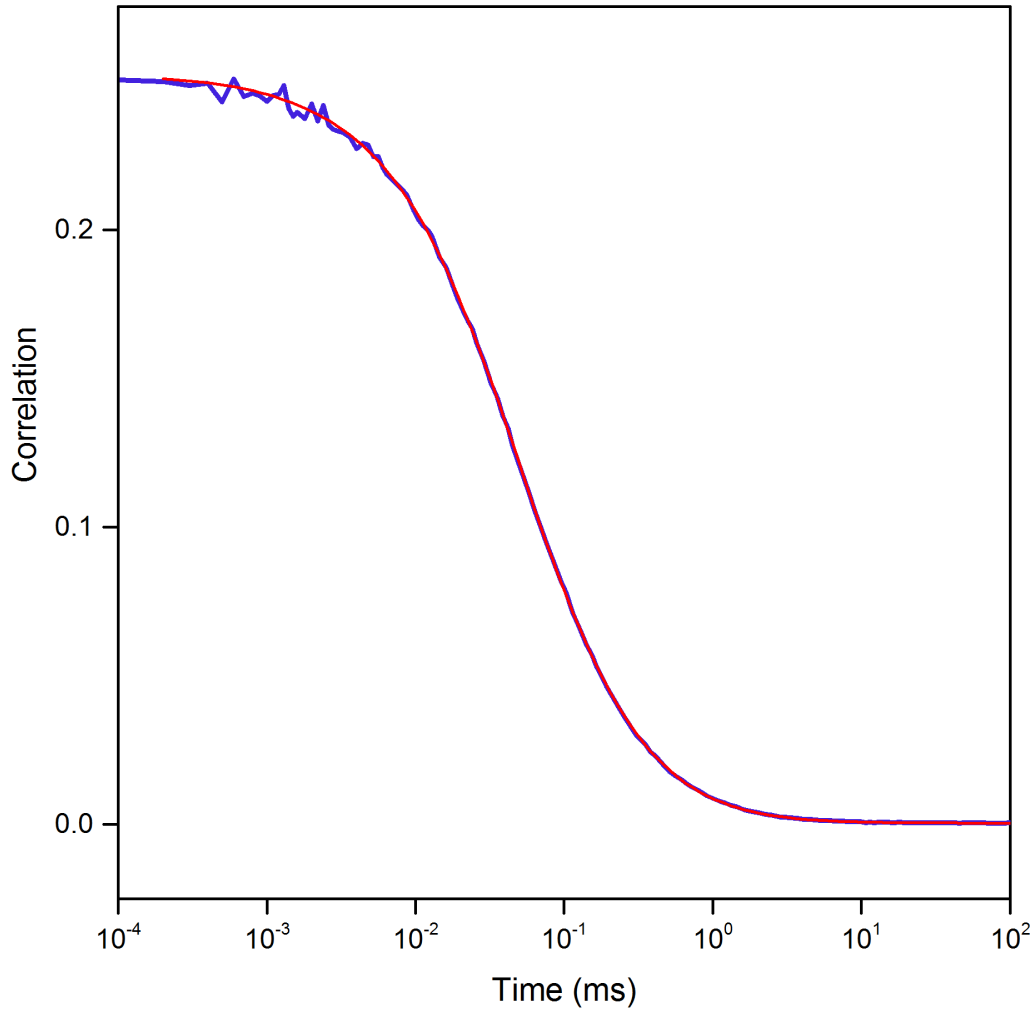

Figure S11. Two-photon FCS measurement (blue line) of rhodamine 110 in water (40 nM). The laser power (transform-limited pulses using the full laser spectrum; see Fig. 9) was 9.4 mW. The red line depicts the fit to the data. Fit parameters: N = 2.79, ω_0/z_0 = 4.4, I_B = 0.6 kHz, S = 130 kHz, τ_D = 49 ± 5 µs.

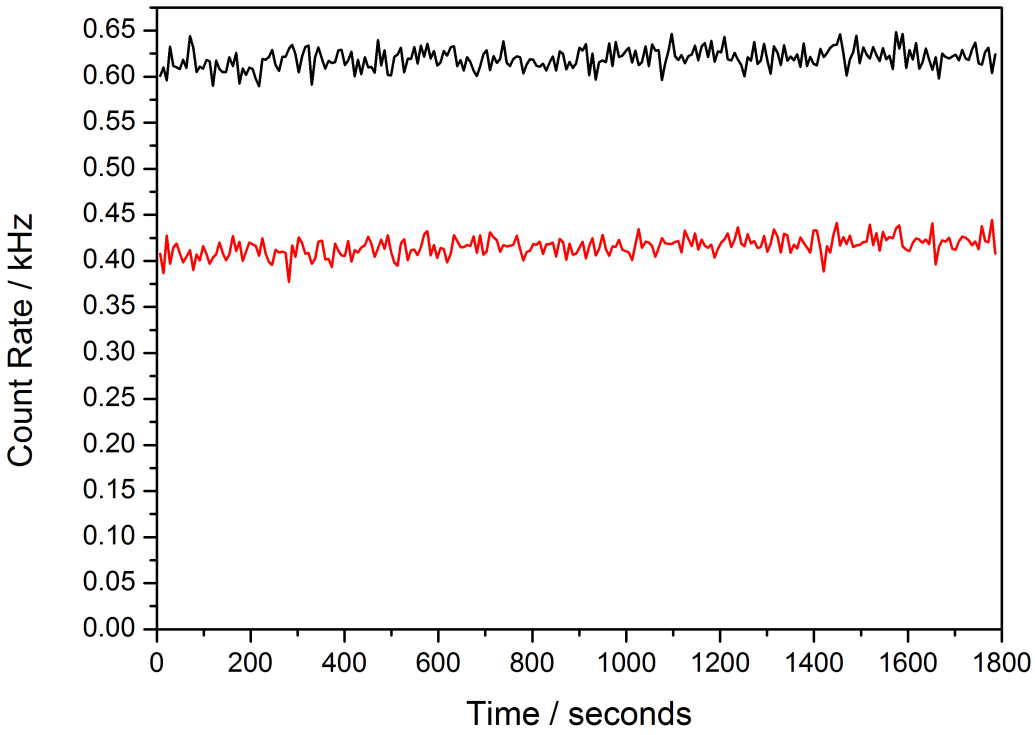

Figure S12. Fluorescence intensity *vs.* irradiation time for pA-containing GA single-strand oligonucleotide, under 2P microscopy conditions. The emission signal is split according to direction of polarization with respect to that of the laser; parallel in black and perpendicular in red. The signal is stable over 30 minutes. Excitation wavelength was 780 nm.

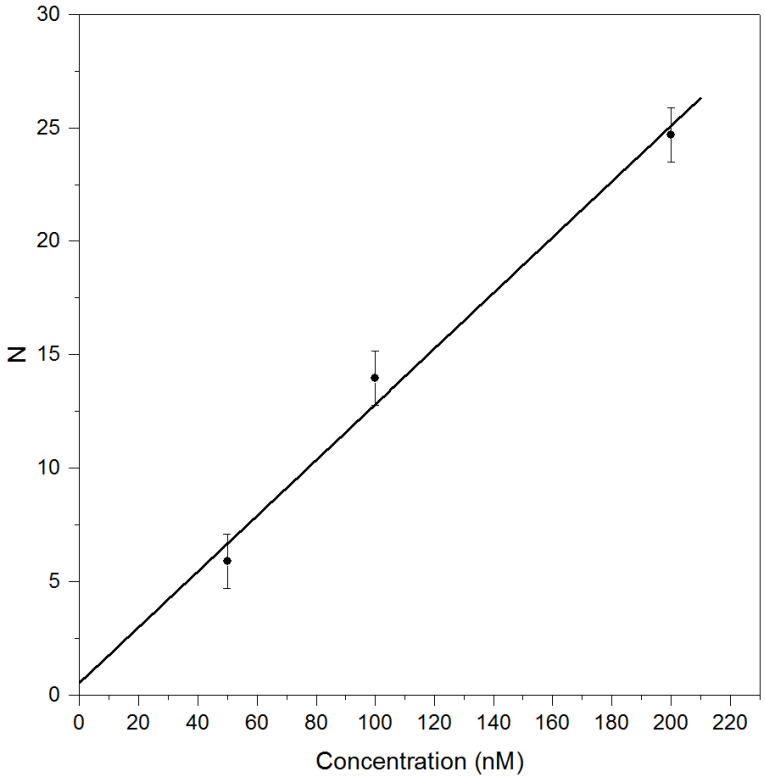

Figure 13. Concentration dependence of the number of molecules of pA-containing GA single-strand oligonucleotide in the excitation volume under 2P microscopy conditions. The number of molecules in the focus, N, was calculated according to equation 6 in the main text. The buffer solution was at 22 ºC and the laser power was 7.1 mW with 30 min integration time for each data point. The error bars are estimated, and correspond to those measured previously at a sample concentration of 54 nM (see main text).

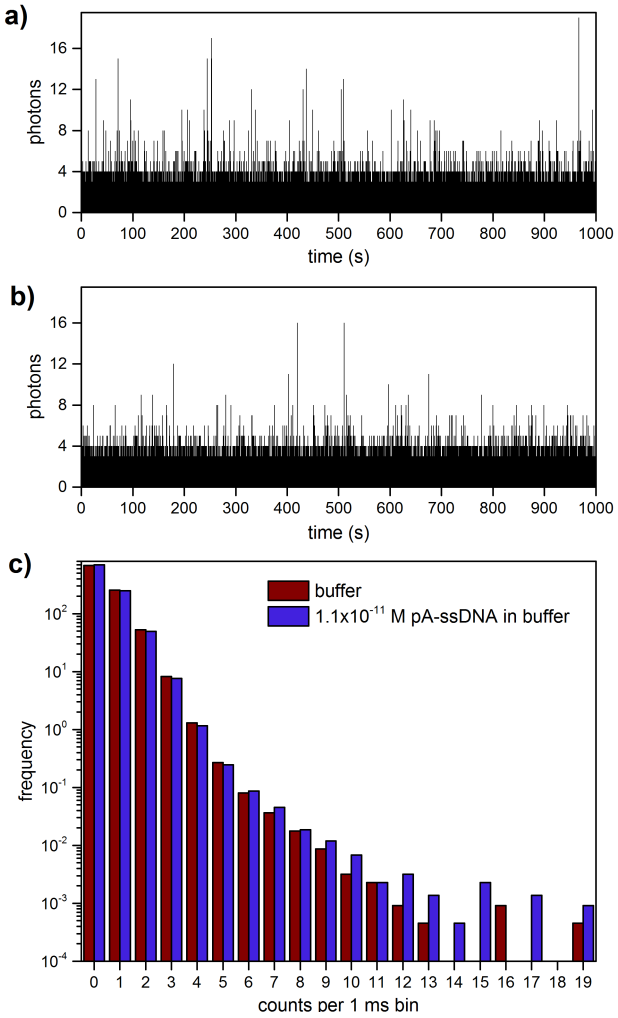

Figure S14. Confocal MCS trace for (a) pA-containing GA single strand oligonucleotide (1.1×10^{-11} M in buffer) and (b) pure buffer; (c) the corresponding photon counting histogram for a 30 minute measurement. The measurement was recorded with a laser power of 10.7 mW and the optimal pulse shape (see main text for details).

SUPPLEMENTARY TABLES

Table S1. Fluorescence decay parameters, fractional contributions to steady-state intensity (SS_i) and average lifetime ($<\tau>$) for pA in phosphate buffer (pH 7.5) and ethanol, excited by 1P-absorption at 390 nm. A-factors (A_i) are shown for an emission wavelength of 430 nm. (Global χ^2 values were 1.07 for pA in PBS and 1.09 in ethanol. Errors in values of lifetimes and A factors $\leq$ 5%,).

Solvent	τ_1 / ns	τ_2 / ns	A_1	A_2	SS_1	SS_2	$<\tau>$ / ns
PBS	0.19	5.97	0.35	0.65	0.02	0.98	3.95
Ethanol	0.16	4.82	0.21	0.79	0.01	0.99	3.84

Table S2. A-factors and average lifetimes, as a function of emission wavelength, for pA riboside in ethanol, excited by 1P-absorption at 390 nm Globally fitted lifetimes: τ_1 = 0.16 ns and τ_2= 4.82 ns.

λ_{em} / nm	A_1	A_2	$<\tau>$ / ns
430	0.21	0.79	3.84
450	0.18	0.82	3.99
470	0.18	0.82	3.99

Table S3. A-factors, fractional contributions to steady-state intensity (SS_i) and average lifetimes ($<\tau>$), as a function of emission wavelength for pA riboside in ethanol, excited by 2P-absorption at 790 nm. Globally fitted lifetimes: τ_1 = 0.10 ns and τ_2= 4.87 ns.

λ_{em} / nm	A_1	A_2	SS_1	SS_2	$<\tau>$ / ns
415	0.73	0.27	0.07	0.93	1.39
425	0.77	0.23	0.09	0.91	1.20
435	0.81	0.19	0.12	0.88	1.01

Table S4. Two-photon cross-sections (σ_2) and brightness ($\sigma_2\phi$), and one-photon absorption coefficients (ε_{390}), quantum yields (ϕ) and brightness ($\varepsilon_{390}\phi$), for pA in single- and double-stranded oligonucleotides. One-photon data were reported previously.[2]

	Single Stranded					Double Stranded				
	σ_2 / GM (780 nm)	ε_{390} / M^{-1} cm^{-1}	ϕ	$\sigma_2\phi$ / GM	$\phi\,\varepsilon_{390}$ / M^{1} cm^{-1}	σ_2 / GM (780 nm)	ε_{390} /M^{-1} cm^{-1}	ϕ	$\sigma_2\phi$ / GM	$\varepsilon_{390}\phi$ / M^{-1} cm^{-1}
GA	3.0	14990	0.42	1.3	6296	2.4	14000	0.14	0.35	1960
GG	2.3	14340	0.28	0.65	4015	2.4	13190	0.13	0.30	1715
AT	2.6	14970	0.15	0.39	2246	2.7	14520	0.17	0.46	2468
CC	2.5	14520	0.04	0.09	523	3.0	12850	0.04	0.13	514
TT	2.5	14110	0.03	0.06	423	2.7	13560	0.11	0.30	1492

REFERENCES

1. S. de Reguardati, J. Pahapill, A. Mikhailov, Y. Stepanenko and A. Rebane, *Opt. Express*, 2016, **24**, 9053-9066.
2. M. Bood, A. F. Füchtbauer, M. S. Wranne, J. J. Ro, S. Sarangamath, A. H. El-Sagheer, D. L. M. Rupert, R. S. Fisher, S. W. Magennis, A. C. Jones, F. Höök, B. T., B. H. Kim, A. Dahlén, L. M. Wilhelmsson and M. Grøtli, *Chem. Sci.*, 2018, **9**, 3494-3502.